Results on 3D Pixel Sensors for the CMS Upgrade at the HL-LHC

Rudy Ceccarelli[a,*] **on behalf of the CMS Tracker Group**

[a]*INFN Firenze, via Sansone 1, Sesto Fiorentino, Firenze, Italy*

E-mail: rceccare@cern.ch

The High Luminosity upgrade of the CERN Large Hadron Collider (HL-LHC) calls for new high-radiation tolerant silicon pixel sensors, capable of withstanding, in the innermost tracker layer of the CMS experiment, fluences up to 1.5×10^{16} $n_{eq}cm^{-2}$ (1 MeV equivalent neutrons) before being replaced. An extensive R&D program aiming at 3D pixel sensors, built with a top-side only process, has been put in place in CMS in collaboration with FBK (Trento, Italy) and CNM (Barcelona, Spain) foundries. The basic 3D cell size has an area of 25×100 μm^2 and is connected to a readout chip through a single, central electrode. A number of sensors were interconnected with the CMS pixel ReadOut Chip (CROC): built in 65 nm technology, the chip will be used in the pixel tracker of the CMS experiment during HL-LHC operations. In this paper the first test beam results of irradiated 3D CROC modules are reported. The analysis of collected data shows excellent performance and hit detection efficiencies close to 99% measured after a fluence of 1×10^{16} $n_{eq}cm^{-2}$ while meeting the noise occupancy requirements of the innermost tracker layer.

10th International Workshop on Semiconductor Pixel Detectors for Particles and Imaging (Pixel2022)
12-16 December 2022
Santa Fe, New Mexico, USA

*Speaker
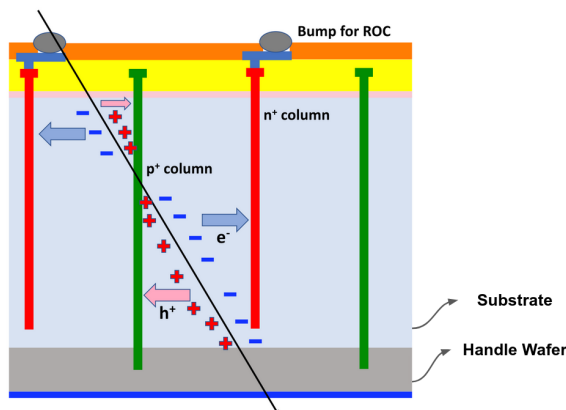
Figure 1: Schematic view of a 3D pixel sensor: the drift path of the charge carriers is highlighted. The substrate is π-type silicon. The handle wafer thickness and electrode spacings are not drawn to scale.

1. Overview

The CMS experiment Phase-2 tracker [1], foreseen for the High Luminosity phase of the Large Hadron Collider (HL-LHC), has two major systems: the Inner Tracker (IT), closer to the collision point and containing pixel detectors, and the Outer Tracker (OT), containing strip and macro-pixel detectors. Pixel detectors will have to withstand very high fluences while preserving high tracking efficiency. Two different technological solutions are available: planar sensors, where the electrodes are parallel to the sensor surface, and 3D sensors, where the electrodes are orthogonal to the sensor surface. In the first case the distance between electrodes is fixed by the sensor's active thickness; in the second case the critical distance is the electrode column spacing, which is typically much shorter than the sensor thickness. Therefore, the bias voltage needed to deplete 3D sensors is smaller with respect to planar sensors. Figure 1 shows a schematic view of a 3D pixel sensor with the drift path of the charge carriers.

The pixel cell size will be $25 \times 100\,\mu\text{m}^2$ in order to have a good spatial resolution, while the total active sensor thickness will be $150\,\mu\text{m}$ in order to keep both the bias voltage and the power dissipation after irradiation at a manageable level, while at the same time allowing for enough collected charge to maintain full hit efficiency. Radiation damage reduces the effective drift distance of charge carriers because of charge trapping, so it is not useful, in the case of planar sensors, to increase the thickness beyond $150\,\mu\text{m}$. In 3D pixel sensors, charge carriers have to travel distances much shorter than the sensor thickness (only $50\,\mu\text{m}$ for a $25 \times 100\,\mu\text{m}^2$ pixel pitch); the trapping probability in irradiated sensors is therefore reduced. Despite the advantages of 3D sensors, the production efficiency is affected by the more complex technology.

In 2022 the CMS collaboration chose planar pixel sensors as the baseline for the IT, although 3D sensors would be used in the innermost barrel layer. Simulations showed that the higher bias voltages needed to deplete highly irradiated planar sensors would lead to thermal runaway after fluences greater than $1 \times 10^{16}\,\text{n}_{\text{eq}}\text{cm}^{-2}$ (1 MeV equivalent neutrons). In any case, the innermost barrel layer is expected to be replaced after a fluence of $\sim 1.5 \times 10^{16}\,\text{n}_{\text{eq}}\text{cm}^{-2}$.

The 3D silicon sensors described in this paper were manufactured by two companies: Fondazione Bruno Kessler (FBK) and Centro Nacional Microtecnologia (CNM). FBK 3D pixel sensors were
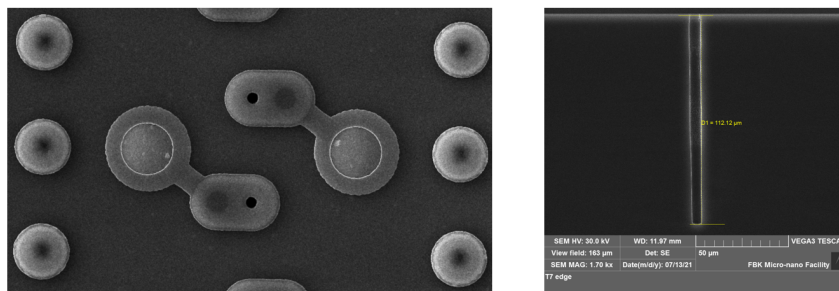
Figure 2: Electron microscope images of FBK 3D sensors: top view of two $25 \times 100\,\mu m^2$ pixel cells (left) and side view of an n^+ column (right).

developed in a collaboration with the Istituto Nazionale di Fisica Nucleare (INFN) [2]. The silicon wafers were produced with the Silicon-Silicon Direct Wafer Bond (DWB) technique. The DWB allows the production of silicon wafers with a thin high resistivity π layer (the substrate) bonded through molecular interactions to a low resistivity p layer (the handle wafer). FBK active devices are implanted on a Float Zone (FZ), high resistivity (> 3000 Ohm cm), 150 μm thick wafer, while the handle wafer is 500 μm thick low resistivity Czochralski silicon. Columnar electrodes of both p^+ and n^+ types are etched by Deep Reactive Ion Etching (DRIE) in the wafer using the Stepper-and-Repeat photo-lithographic technology (with a single-sided process). While the p^+ columns are at least 150 μm long, in order to reach the backside of the sensor, the n^+ columns are shorter: 115 ± 5 μm for FBK sensors. A temporary metal layer was used for sensor testing at FBK and was subsequently removed. In Figure 2, two electron microscope images of FBK 3D sensors are shown: a top view of two $25 \times 100\,\mu m^2$ pixel cells (left) and a side view of an n^+ column (right).

CNM 3D pixel sensor production is very similar with respect to FBK sensors. The main differences are a larger column diameter (8 μm instead of 5 μm), longer n^+ columns (130 μm instead of 115 μm), and the p-stop pixel isolation technique instead of the p-spray technique employed by FBK.

After fabrication, the pixel sensor wafers were processed for UBM (Under Bump Metallization), thinned, diced, and bump-bonded to the CROC readout chips at IZM (Berlin, Germany). The plan is to use the CROC for HL-LHC pixel readout. Built in 65 nm technology, it has 145152 readout channels (432 rows and 336 columns with a bump pad pitch of $50 \times 50\,\mu m^2$). The CROC is the second iteration, specific to the CMS experiment, of the RD53 project, which is a joint effort between the CMS and ATLAS collaborations to develop a pixel readout chip for the HL-LHC [3]. The first iteration of the chip was the RD53A, which was half the size of CROC and was used for pixel sensors R&D until the beginning of 2022.

The sensor plus chip assembly is referred to as a "pixel module" in the following.

2. Irradiation Campaign and Test Beam Experiment

In order to verify that both the sensor and the readout chip are able to withstand the high fluences expected during HL-LHC operations with a minimum loss of performance, pixel modules are usually tested before and after irradiation. The pixel modules studied in this paper (two FBK 3D and one CNM 3D) were irradiated in a 24 GeV/c proton beam at the CERN IRRAD facility in
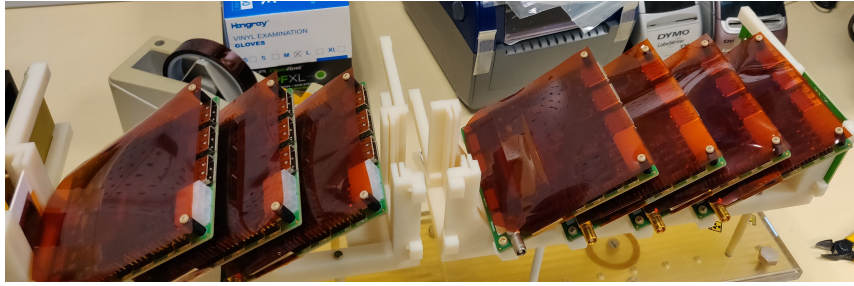
Figure 3: Photograph of the mechanical support employed to irradiate the three 3D modules (two FBK and one CNM) in the CERN IRRAD facility.
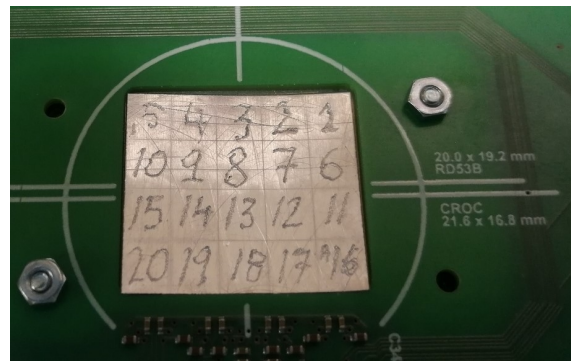

Figure 4: Photograph of one of the aluminum foils placed behind the modules to be irradiated, employed to estimate the fluence after irradiation. The cut lines for the 20 smaller pieces are visible.

September 2022. The irradiation support with the modules mounted on it is shown in Figure 3. The modules were inclined by 30° with respect to the beam in order to achieve a uniform vertical irradiation (the beam FWHM is of the order of 10 mm in both directions). Moreover, it was possible to continuously move the support structure so as to irradiate a larger area with the beam.

In order to estimate the irradiation fluence the modules received, aluminum foils were placed behind the modules, as shown in Figure 4. The aluminum foils were cut into 20 smaller pieces (about $5 \times 5 \, \text{mm}^2$) after irradiation, in order to estimate the fluence in different regions of the pixel module using spectroscopy. The measurements showed that the irradiation was horizontally uniform, but not vertically centred. However, more than one third of the pixel module was irradiated to $1 \times 10^{16} \, \text{n}_{eq}\text{cm}^{-2}$; this area is referred to as the Region of Interest (ROI) in the following. Finally, the measurements were consistent between the aluminum foils placed behind the different pixel modules.

The irradiated 3D modules were tested in a 120 GeV/c pion beam at the CERN SPS test beam facility in November 2022. The test beam area is equipped with an EUDET telescope [4]: it is made of six planes of monolithic pixel detectors, featuring MIMOSA-26 (M-26) sensors, manufactured with the 350 nm CMOS technology. The M-26 sensors consist of 1152 columns and 576 rows of pixels with $18.4 \times 18.4 \, \mu\text{m}^2$ pitch, covering an active area of $21.2 \times 10.6 \, \text{mm}^2$. The three irradiated 3D modules, which will be referred to as Devices Under Test (DUTs) in the following, were kept inside a cooling box placed in the middle of the telescope. The air inside the box was kept at -30 °C. The DUTs could be rotated with respect to the beam, in order to acquire data for tracks inclined
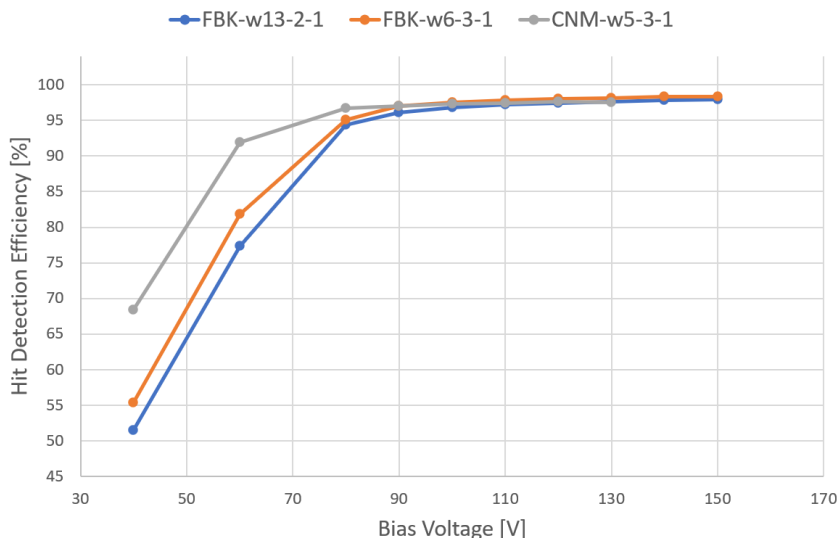
Figure 5: Hit detection efficiency as a function of the bias voltage for the three DUTs. The pixel thresholds were tuned to an average value of 1000 electrons for all DUTs. The results refer to a ROI with a uniform irradiation of 1×10^{16} $n_{eq}cm^{-2}$. The wZ-X-Y notation indicates the X-Y position of the sensor in the wafer Z of the production (either FBK or CNM).

with respect to the DUTs.

3. Test Beam Results

The three DUTs were tuned to average pixel thresholds of 1000 electrons, with a dispersion of about 100 electrons. The hit detection efficiency of the DUT was calculated from the intersection of telescope trajectories with the DUTs, with a search window of at least twice the pixel pitch. As mentioned before, a ROI was defined in order to select an area of uniform irradiation (about 1×10^{16} $n_{eq}cm^{-2}$) for each DUT: only particle tracks falling inside this ROI were considered for the results presented in this paper.

Figure 5 shows the hit detection efficiency of the three DUTs as a function of the bias voltage, for orthogonal beam incidence. The efficiency plateau is about 60 V wide and starts around 90 V. The CNM module appears to be more efficient at lower bias voltages, probably thanks to a better threshold tuning.

All three modules achieve a maximum hit efficiency ($\sim 98\%$) at a bias voltage of 130 V. It should be noted that, since the sensor columns contain passive material, when the beam is orthogonal to the DUTs the hit detection efficiency is lower at the column boundaries. Therefore, it is not possible to achieve 100% efficiency with orthogonal beam incidence.

Because of the combination of high irradiation and low thresholds, some pixel channels can become noisy. Pixel channels with a noise occupancy exceeding 2×10^{-5} were tagged as noisy and were masked in data acquisition and data analysis. This threshold corresponds to 1% of the expected occupancy in the first barrel layer of the CMS IT during HL-LHC operations.

Figure 6 shows the fraction of the noisy pixel channels as a function of the bias voltage for the three
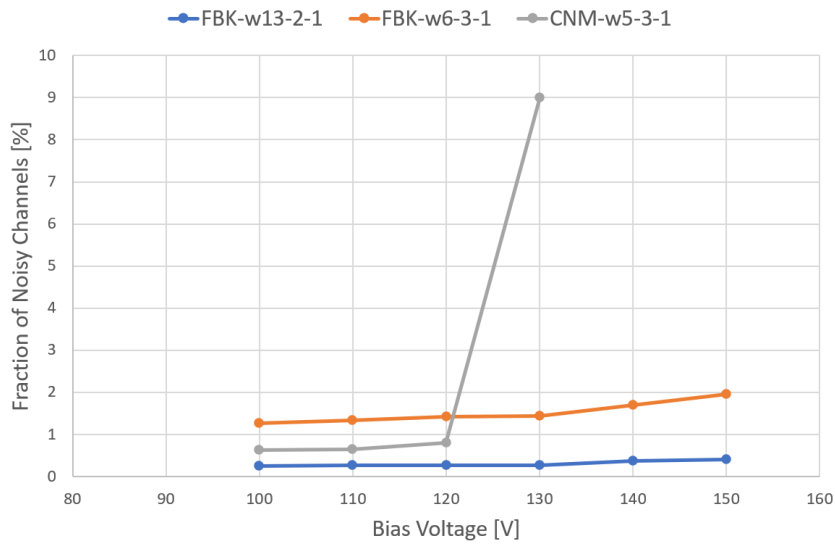
Figure 6: Fraction of noisy pixel channels as a function of the bias voltage for the three DUTs. The pixel thresholds were tuned to an average value of 1000 electrons for all DUTs. The results refer to a ROI with a uniform irradiation of 1×10^{16} n_{eq}cm^{-2}.
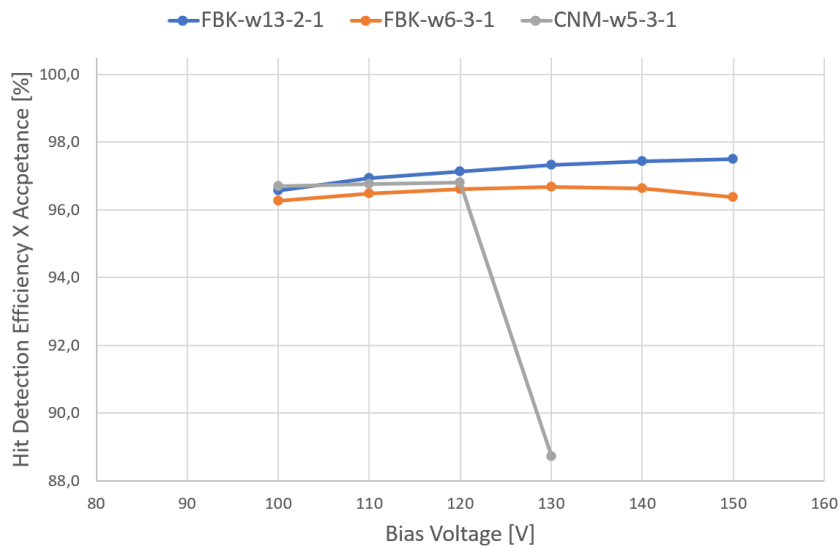
Figure 7: Hit detection efficiency times acceptance as a function of the bias voltage for the three DUTs. The pixel thresholds were tuned to an average value of 1000 electrons for all DUTs. The results refer to a ROI with a uniform irradiation of 1×10^{16} n_{eq}cm^{-2}.
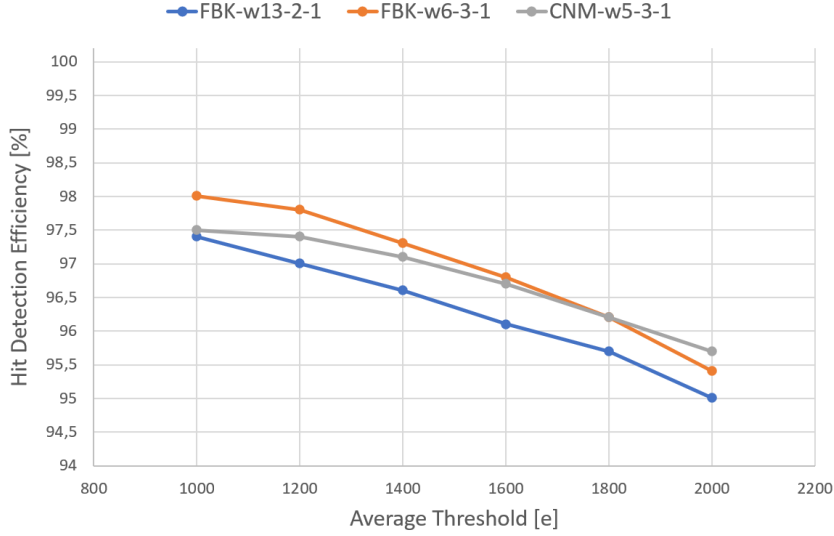
Figure 8: Hit detection efficiency as a function of the average pixel threshold for the three DUTs. The FBK modules were operated with a bias voltage of 130 V, while the CNM module was operated at 120 V. The results refer to a ROI with a uniform irradiation of 1×10^{16} $n_{eq}cm^{-2}$.

DUTs. The two FBK modules are stable up to 150 V, but for the CNM module a steep increase of the noisy channels can be observed above 120 V. The cause is still under investigation, and it was observed also with irradiated FBK sensors interconnected with the RD53A readout chip [5]. A possible explanation of the different behavior between CNM and FBK sensors is related to the length of n^+ columns: in CNM sensors they are about 15 μm longer with respect to FBK sensors. The average pixel threshold can have a large impact on the number of noisy channels. The CNM module was retuned to a higher threshold of 1200 electrons: with the new tuning the number of noisy channels decreased to 2% at 130 V.

In order to present a more practical hit detection efficiency, that takes into account the number of masked channels, the acceptance can be defined as:

$$\text{Acceptance} = 1 - \frac{\text{Number of Noisy and Stuck Channels}}{\text{Number of Channels}} \tag{1}$$

where stuck channels are defined as pixels that do not respond to charge injections (they are also masked in data acquisition and data analysis). Figure 7 shows the hit detection efficiency times the acceptance as a function of the bias voltage: the effect of the large number of noisy channels can be observed for the CNM module. However, it should be noted that the CNM module can be operated with high efficiency between 90 and 120 V, with a moderate number of noisy channels.

The three DUTs were tuned again to higher thresholds in order to evaluate the effect of the pixel threshold on the hit efficiency. Figure 8 shows the hit detection efficiency as a function of the pixel threshold. The two FBK modules were operated at a bias voltage of 130 V, while the CNM module was operated at 120 V. It can be observed that doubling the threshold lowers the hit efficiency by approximately 2.5%. With a pixel threshold of 2000 electrons the hit efficiency reaches a minimum value of 95% for one DUT.

Finally, the hit efficiency was studied also as a function of the turn angle: the DUTs were rotated
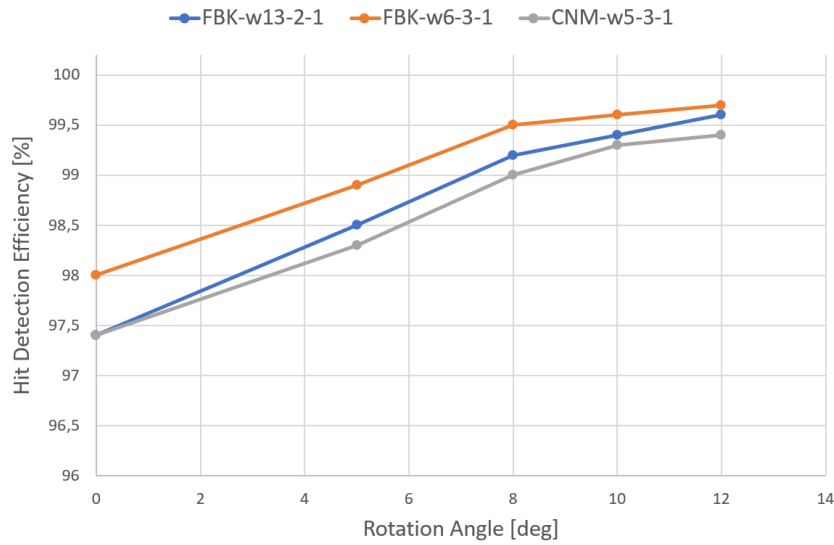
Figure 9: Hit detection efficiency as a function of the turn angle for the three DUTs. The pixel thresholds were tuned to an average value of 1000 electrons for the FBK modules and 1200 electrons for the CNM module. The FBK modules were operated with a bias voltage of 130 V, while the CNM module with a bias voltage of 120 V. The results refer to a ROI with a uniform irradiation of $1 \times 10^{16}\, n_{eq}cm^{-2}$.

with respect to the beam around the 25 μm pitch. The measured hit efficiency for rotated 3D sensors should be higher since incident particles will no longer be fully contained within the passive material of a column. Figure 9 shows the hit detection efficiency as a function of the turn angle. The pixel thresholds were tuned to an average value of 1000 electrons for the FBK modules and 1200 electrons for the CNM module. Also in this case, the two FBK modules were operated at a bias voltage of 130 V, while the CNM module was operated at 120 V. For all DUTs an efficiency greater than 99% can be obtained with a turn angle greater than 8°.

4. Summary

This paper shows the first test beam results of irradiated 3D CROC modules, which will be used in the innermost layer the CMS HL-LHC Inner Tracker barrel section. The modules were irradiated to a fluence of $1 \times 10^{16}\, n_{eq}cm^{-2}$ and show excellent performances: the hit detection efficiency plateau starts around 90 V and it is about 60 V wide, at least for the FBK modules. The CNM module suffered an increase in the number of noisy pixel channels above a bias voltage of 120 V, but could be operated nonetheless between 90 and 120 V with a high hit detection efficiency.

The presented results are compatible with previous measurements of 3D RD53A modules irradiated up to $1.8 \times 10^{16}\, n_{eq}cm^{-2}$ [5]. During 2023 further irradiations are planned, in order to qualify 3D CROC modules up to $1.5 \times 10^{16}\, n_{eq}cm^{-2}$, which is the target fluence for replacing the innermost barrel layer of the CMS Inner Tracker.

References

[1] The CMS Collaboration, *The Phase-2 Upgrade of the CMS Tracker*, CERN-LHCC-2017-009, CERN, 2017.

[2] G.F. Dalla Betta et al., *Small pitch 3D devices*, PoS(Vertex 2016) 028, 2016.

[3] M. Garcia-Sciveres, *The RD53A Integrated Circuit*, CERN-RD53-PUB-17-001, CERN, 2017.

[4] H. Jansen, S. Spannagel, J. Behr et al., *Performance of the EUDET-type beam telescopes*, EPJ Techniques and Instrumentation 3, 7, 2016.

[5] R. Ceccarelli (on behalf of the CMS Tracker Group), *Performance of highly irradiated FBK planar and 3D pixel detectors*, Nuclear Inst. and Methods in Physics Research A Vol. 1046 167650, 2022.